

## Electrodeposition of Fe-Ni-Cr alloy from Deep Eutectic System containing Choline chloride and Ethylene Glycol

Gengan Saravanan, Subramanian Mohan\*

Electroplating and Metal Finishing Technology division  
CSIR-Central Electrochemical Research Institute  
Karaikudi – 630006, India

\*E-mail: [sanjnamohan@yahoo.com](mailto:sanjnamohan@yahoo.com)

Received: 22 September 2010 / Accepted: 20 January 2011 / Published: 1 May 2011

---

A novel procedure for the electrochemical deposition of Fe-Ni-Cr alloy was investigated on mild steel substrate. The alloy contains approximately 53-61% Fe, 34-41% Ni, and 4-15% Cr, our results show that it is possible to produce a thick deposit of the alloy. The influence of electrodeposition potential upon the Fe, Ni, and Cr composition were investigated. Surface morphology and composition of deposits were analyzed using SEM with EDAX. The corrosion resistance of Fe<sub>54.62</sub>Ni<sub>30.87</sub>Cr<sub>14.5</sub> electrodeposited alloy on mild steel substrate were determined and compared with simulated data.

---

**Keywords:** Alloy (A), stainless steel (A), EIS (B), SEM (B), electrodeposited films (C).

### 1. INTRODUCTION

Fe-Ni-Cr alloy is a widely used in many areas due to its good corrosion resistance, magneto-resistive, and mechanical properties [1-4]. Resistance towards aggressive media and its biocompatibility would make the alloy an excellent candidate for developing cheap biodevices, [5] composition equivalent to stainless steel is reported by M.R. El-Sharif et al. [6-7] and it would allow advantage to aforementioned properties and for fabrication of electroformed structures with complex shapes. Electrodeposition of alloy such as Fe-Cr [8], Fe-Ni-Cr [7, 9], and Fe-Ni-Cr-Mo [10], has been reported in the literature but were limited to producing thin layers in aqueous based electrolytes. Due to the complexity of producing a ternary alloy by electrochemical means, the presence of Cr in high quantity in the deposits is a challenge by itself [11]. First of all, Cr(III) aqua-species, Cr(H<sub>2</sub>O)<sub>6</sub><sup>3+</sup>, being a very strong Lewis acid, undergoes a rapid olation reaction between unprotonated forms in aqueous electrolyte, annihilating Cr deposition. To prevent this phenomenon, we will be investigating Cr

electrodeposition from DES based on choline chloride without any complexing agent [12]. Additionally, the presence of Cr in the alloy decreases the quality of the structure by the formation of cracks, low thickness, and increase of internal stress. In order to overcome this problem, the addition of an organic additive such as saccharine [13] will reduce the stress and may help to get a better deposits quality. On the other hand, these additives are known to prevent the formation of a passivated oxide layer at the surface, thereby decreasing the corrosion resistance of the alloy [14]. In aqueous based electrolyte, the reduction of water into hydrogen runs with very low overpotential on transition metal [15] deposits and leads to free H<sub>2</sub> and OH<sup>-</sup> anions. This reduction of water decreases the cathode efficiency and the hydroxide increases the pH, which precipitates the iron and nickel as their insoluble hydroxides. The precipitation of Cr(III) species into the deposits is also a problem [16].

In this study, a novel DES based electrolyte is developed allowing the deposition of Fe-Ni-Cr alloys [17]. This work is very important in terms of free from aqueous electrolyte, complexing agent, additive like saccharine and H<sub>2</sub> reduction. Effect of electrodeposition potential on the composition, structural morphology, and corrosion resistance properties of alloy deposits were investigated.

## 2. EXPERIMENTAL SECTION

### 2.1. Preparation of Deep Eutectic Solvent and Electrochemical Deposition

The deep eutectic solvent (DES) was prepared by mixing choline chloride – 4.4 g, CrCl<sub>3</sub>·6H<sub>2</sub>O – 8.5 g, NiCl<sub>2</sub>·6H<sub>2</sub>O – 3.8 g, FeSO<sub>4</sub>·7H<sub>2</sub>O - 0.33 g, KCl – 1.5 g, ethylene glycol – 44.4 g, at 65°C until a homogeneous, green liquid was formed [18]. Potentiostatic electrodeposition was carried out using three electrode cell connected to a potentiostat/galvanostat PARSTAT 2273. Constant potential deposition was carried out in an undivided cell at potential from -1.3 to -1.5 V. The working electrode (area, 1cm<sup>2</sup>) was either copper or mild steel, counter and reference electrode were platinum foil and saturated calomel electrode directly immersed in DES. The sample was degreased in acetone, electro cleaned in alkaline solution, rinsed with 5% H<sub>2</sub>SO<sub>4</sub> and finally rinsed with double distilled water.

### 2.2. Microchemical and Microstructural analyses

Structural morphology and elemental composition of deposits were carried out using scanning electron microscopy energy dispersive X-ray spectroscopy (Hitachi, 3000H). X-ray diffraction pattern of alloy phases were measured using a Phillips diffractometer, 2θ from 20 to 100 using CuKα, λ = 0.1540 nm.

### 2.3. Corrosion resistance studies

The electrochemical measurements were carried out using a PARSTAT 2273 advanced electrochemical system (Princeton Applied Research Company, USA). A saturated calomel electrode (SCE) was used as the reference electrode and a large platinum plate as the counter electrode. The mild

steel (MS) and Fe-Ni-Cr alloy obtained at -1.5 V on MS were the working electrodes. The corrosive medium in the test was 3.5% NaCl aqueous [19]. Potentiodynamic polarization curves were measured for both substrate and electrodeposited alloy between -0.25 and 0.25V at scan rate of 5 mV/s. The corrosion parameters were obtained with inbuilt software package (Power Suite). EIS were conducted at open circuit potential over a frequency range from  $10^5$  to  $10^{-2}$  Hz. The amplitude of potential modulation was 5 mV. All the recorded impedance spectra were shown as Nyquist diagram. ZSimpWin (3.21) software was used to fit the EIS experimental data.

### 3. RESULT AND DISCUSSION

#### 3.1. X-ray diffraction analysis

Figure.1 shows a typical X-ray diffractogram for the electrodeposited alloy. As can be seen, this alloy exhibits sharp lines characteristic for poly crystalline nature. The peaks were observed at diffraction angle of 43.4, 50.4, 73.9, 89.8 and 94.9° corresponding to (111), (200), (220), (311) and (222) crystal planes and Fe-Ni-Cr phases were polycrystalline. All peaks can be indexed as the Fe-Ni-Cr face-centered cubic (FCC) phases based on the standard data of the JCPDS (Card no. 33-0945) file. The average crystallite size was estimated at 35.5 nm using Scherer formula [20, 21].

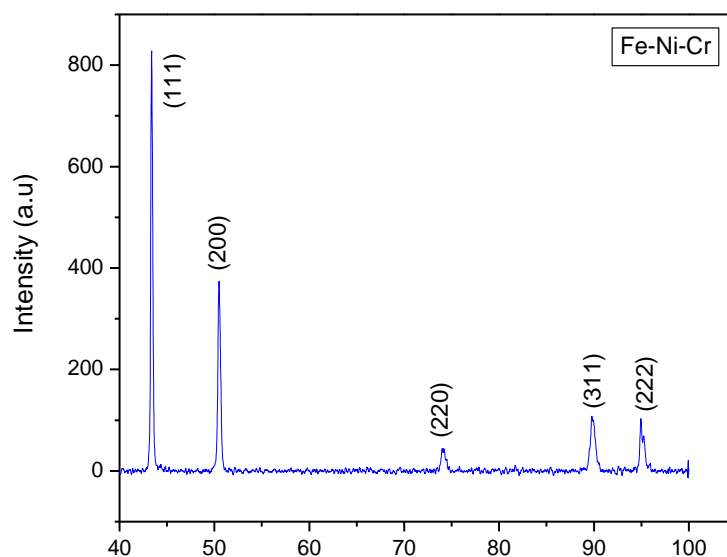


**Figure 1.** XRD pattern of Fe-Ni-Cr alloy deposited at -1.5 V in deep eutectic solvent based on choline chloride and ethylene glycol.

#### 3.2. Microstructural characteristics and elemental composition

Deposition potential has an important effect on deposit brightness, microstructure and composition of alloy deposits on copper substrate. In the present studies, the SEM images and EDAX

patterns show differences on the samples obtained by potentiostatic deposition technique. Fig. 2A and 2B shows the morphology of alloy deposited at -1.3V and the corresponding EDAX pattern reveals the presence of Fe-53.7% Ni- 41.7% and Cr-4.5%. Deposits were darker than one obtained at -1.4 and -1.5V, nodular grain sizes ranging from 0.3-0.7µm with agglomeration of particles formed are seen.

Fig. 2C and 2D shows the SEM and EDAX results of alloy obtained at -1.4V, these deposits were brighter than those obtained at -1.3V with grain sizes ranging from 0.2-0.5µm. Deposits were denser and compact layer containing spherical particles were formed as small clusters. The compositions of alloy atomic percentage were Fe-60.9% Ni-34.3% and Cr-4.7% as shown by EDAX analysis. SEM and EDAX results of alloy deposits obtained at -1.5V and these results were shown in Fig. 2E and 2F. Deposits were brighter, homogeneous, dense and very small nodular grains with an average size of 0.2µm. Bright deposits could be due to increasing of Cr percentage in the alloy composition, EDAX shows that the atomic percentages of alloy were Fe-54.6%, Ni-30.8% and Cr-14.5%.

From the analysis of alloy deposits morphology and composition under different potentials, it appears that the type of deposits and composition gradually changed from darker to bright and from distorted [22] to close stainless steel [23] compositions [24].

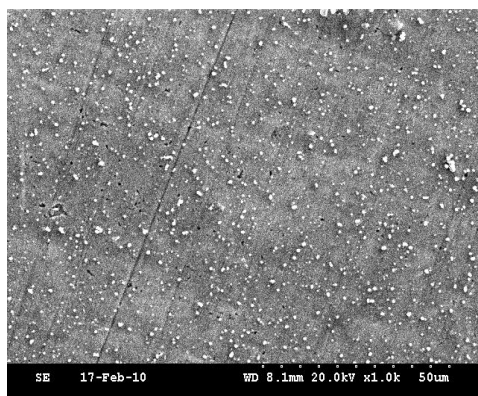


Figure 2. (A) SEM

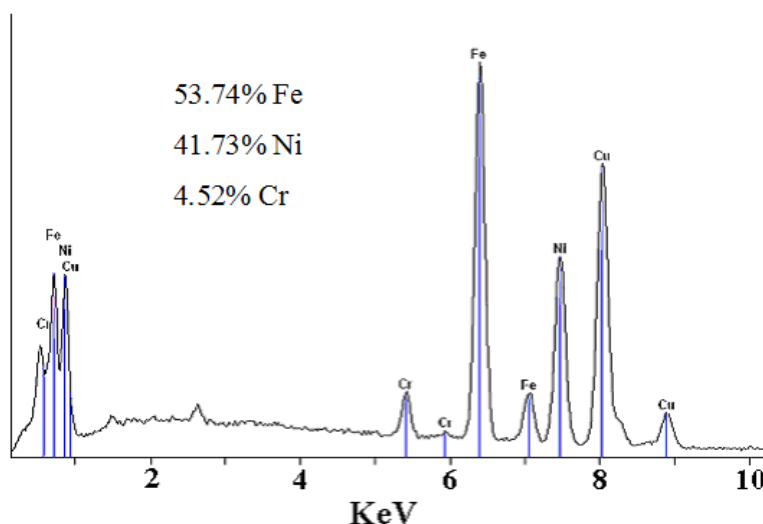


Figure 2. (B) EDAX

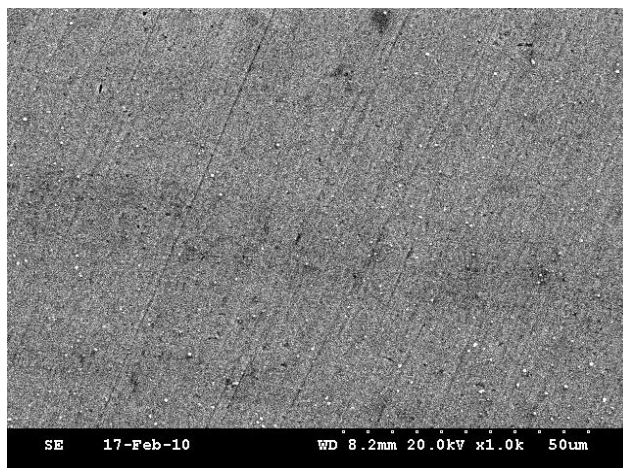


Figure 2. (C) SEM

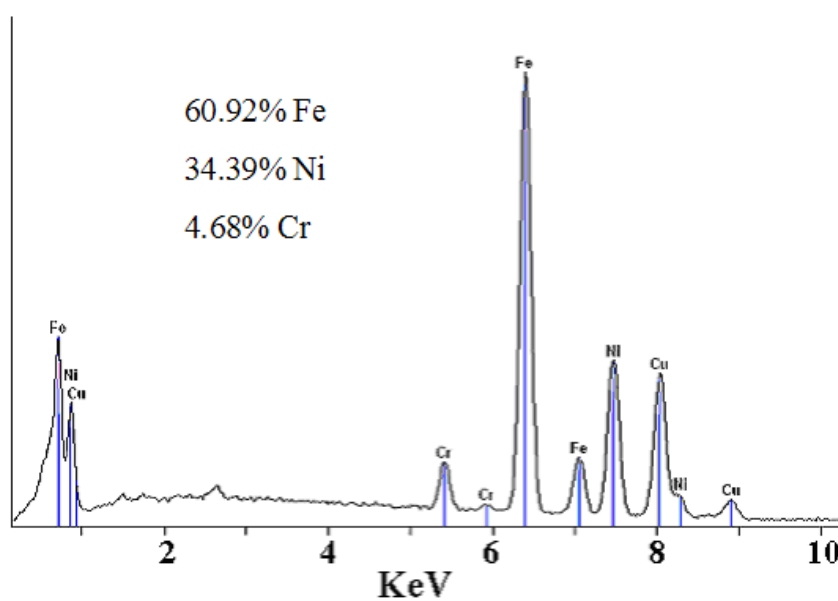


Figure 2. (D) EDAX

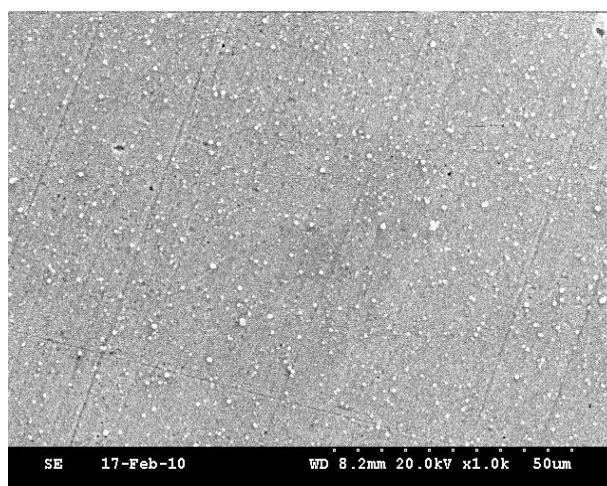


Figure 2. (E) SEM

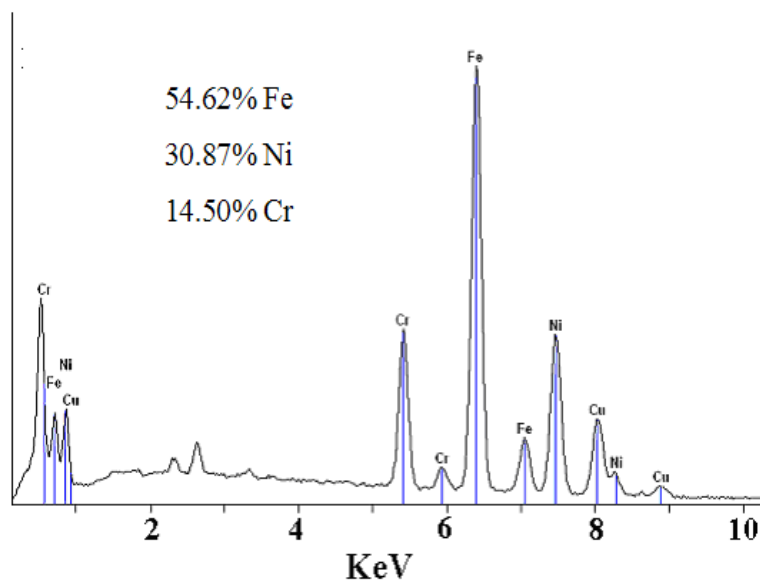


Figure 2. (F) EDAX

**Figure 2.** SEM images and EDAX patterns of Fe-Ni-Cr alloy deposits prepared under different conditions: (2A and 2B)  $\text{Fe}_{53.74}\text{Ni}_{41.73}\text{Cr}_{4.52}$  electrodeposited alloy at -1.3 V; (2C and 2D)  $\text{Fe}_{60.92}\text{Ni}_{34.39}\text{Cr}_{4.68}$  electrodeposited alloy at -1.4 V; (2E and 2F)  $\text{Fe}_{54.62}\text{Ni}_{30.87}\text{Cr}_{14.5}$  electrodeposited alloy at -1.5 V.

The electrical double layer structure in DES may be expected to be different from that in the conventional media containing molecular solvent dipole and supporting electrolyte, because DES is composed of ions and they are directly in contact with the electrode surface. Compact-layer effect [25, 26] on the electrical double layer structure in DES would facilitate diffusion of ions.

### 3.3. Potentiodynamic polarization tests

The results from the potentiodynamic polarization measurements of the  $\text{Fe}_{54.62}\text{Ni}_{30.87}\text{Cr}_{14.5}$  alloy deposits on the mild steel substrate in 3.5% NaCl aqueous solution are shown in Fig. 3A. The curves representing the mild steel (MS) and a  $\text{Fe}_{54.62}\text{Ni}_{30.87}\text{Cr}_{14.5}$  electrodeposits obtained at -1.5V on mild steel were shown for comparison. The earlier studies [27-29] indicate that transpassivation is always accompanied by an increase in the anodic current density. In most cases, it is consider that the indication of the onset of transpassivation is a sudden increase in the anodic current density with increasing electrode potential. As Fig. 3A shows, the current density of the Fe-Ni-Cr deposits increased rapidly when the potential reached -0.146 V (SCE), and there is no obvious localized corrosion on the surface of alloy deposits. Therefore it is proposed that transpassivation of alloy deposits occurs at this potential. In the whole transpassive region the current density of the alloy deposits is much smaller than that of the mild steel substrate. It is clear from a comparison of the corrosion potential ( $E_{corr}$ ) of the mild steel substrate -0.671 V (SCE) with the application of the  $\text{Fe}_{54.62}\text{Ni}_{30.87}\text{Cr}_{14.5}$  alloy deposits, reaching -0.385V (SCE). This increasing  $E_{corr}$  indicates that after applying an alloy deposits a better corrosion protection is obtained. Corrosion protection is normally

proportional to the corrosion current density ( $I_{corr}$ ) measured via polarization. The very lower ( $I_{corr}$ ) values for the Fe<sub>54.62</sub>Ni<sub>30.87</sub>Cr<sub>14.5</sub>/mild steel ( $1.1 \times 10^{-5}$ ) [23] than that of bare mild steel ( $71 \times 10^{-5}$ ) could indicate that the Fe<sub>54.62</sub>Ni<sub>30.87</sub>Cr<sub>14.5</sub> alloy electrodeposits is more protective than the mild steel substrate. Corrosion rate in mmpy was estimated from the polarization curves, and is given in Table.1. Very lower corrosion rate is obtained for alloy deposits than that of bare substrate.

**Table 1.** Corrosion parameters obtained from potentiodynamic polarization and electrochemical impedance measurements by Nyquist plot in 3.5% NaCl solution.

Sample	$E_{corr}$ V (SCE)	$b_a$ (V/decade)	$b_c$ (V/decade)	$I_{corr}$ (A/cm <sup>2</sup> )	Corrosion rate (mmpy)	$R_{ct}$ (Ω/cm <sup>2</sup> )	$Z_w$ (Ω/cm <sup>2</sup> )	$C_{dl}$ (F/cm <sup>2</sup> )	Porosity (%)
MS substrate	-0.671	0.373	-0.061	$7.1 \times 10^{-4}$	8.42	116	-	$1.0 \times 10^{-3}$	-
FeNiCr/mild steel	-0.384	0.228	-0.260	$1.1 \times 10^{-5}$	0.1213	3053	287	$1.7 \times 10^{-3}$	0.2237

### 3.4. Electrochemical impedance spectroscopy measurements

The polarization resistance and double layer capacitance of Fe-Ni-Cr deposits in a corrosive medium could provide information regarding the ongoing corrosion reaction process. EIS data provides additional information about the deposits/solution and substrate/solution interface. The simple RC combination can be used to model several components of an electrochemical cell. For example, the bulk electrolyte and a deposits on the electrode surface each has an associated resistance and capacitance. However, it should be noted that the semi-circle for the bulk electrolyte is often not seen since it typically occurs at higher frequencies than those that can be used in an impedance experiment. Therefore, only the low frequency limit can be measured. This parallel combination can also be used to model the interfacial region;  $C$  is double-layer capacitance ( $C_{dl}$ ) and  $R$  is the charge transfer resistance ( $R_{ct}$ ). The rationale for representing the charge-transfer reaction as a resistance is derived from the small overpotential limit of the Butler-Volmer equation [30, 31]

$$i = i_0 \left( -\frac{nFA}{RT} \right) \eta$$

Where  $R_{CT} = RT/i_0 nFA$

It should be stressed that this linear relationship only applies at low overpotentials between 5 to 10 mV. Hence, the A.C. amplitude used in electrochemical impedance experiments is limited to 5 to 10 mV. The other fundamental component of an electrochemical cell that must be considered is mass-transport. Semi-infinite diffusion can be modeled using the Warburg impedance  $Z_w$ , which is given by the following equation.

$$Z_w = \frac{\omega}{\sqrt{j\omega}}$$

This element has a constant phase angle and yields a straight line in the Nyquist plot at an angle of 45°. The equivalent circuit for an electrochemical cell, in which solution species involved in the charge-transfer reaction can be constructed from the components discussed above, is shown as insert in Fig. 3B and 3C. The semi-circle at high frequencies indicates charge-transfer control; however, at lower frequencies, the rate of mass-transfer become the rate limiting factor and is reflected by the transition from a semi-circle to a straight line.

Fig. 3B and 3C shows the experimental and simulated impedance response of bare mild steel and Fe-Ni-Cr alloy deposits on mild steel substrates in a Nyquist representation. At low frequencies the interception with the real axis was ascribed to the charge transfer resistance  $R_{ct}$  at the corrosion potential. The  $R_{ct}$  value of  $Fe_{54.62}Ni_{30.87}Cr_{14.5}/mild\ steel$  was several order magnitude higher than that of bare mild steel substrate. The value of fitted parameters of the equivalent circuit, together with the corrosion potentials  $E_{corr}$  as a function of  $Fe_{54.62}Ni_{30.87}Cr_{14.5}$  alloy electrodeposits on mild steel substrate were presented in Table.1. Porosity of  $Fe_{54.62}Ni_{30.87}Cr_{14.5}$  alloy electrodeposits on mild steel substrate were calculated based on our previous studies [32, 33]. Table 1 shows that the diffusion impedance value ( $Z_w = 287 \Omega/cm^2$ ) of the deposited alloy is higher than the charge-transfer resistance of mild steel substrate ( $R_{ct} = 116 \Omega/cm^2$ ). This shows that diffusion process can dominate the whole corrosion process for the deposited alloy and also means that the uncoated mild steel substrate easily suffers from attack by aggressive substance like  $CO_2$  and chloride ions. Both  $R_{ct}$  and  $Z_w$  values of the deposited alloy are much larger than those of the bare mild steel substrate. This suggests that electrochemical reaction is difficult on the deposited electrode surface and Fe-Ni-Cr alloy deposits presents better corrosion resistance.

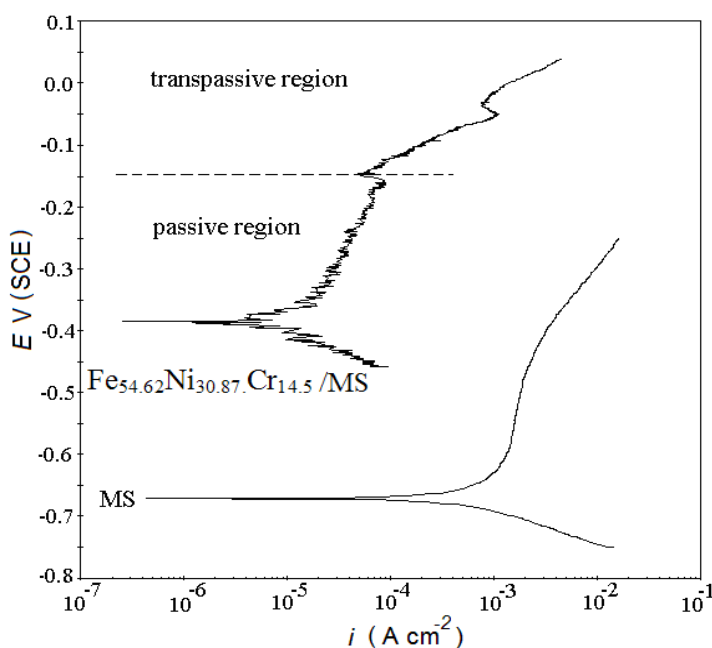


Figure 3. (A)

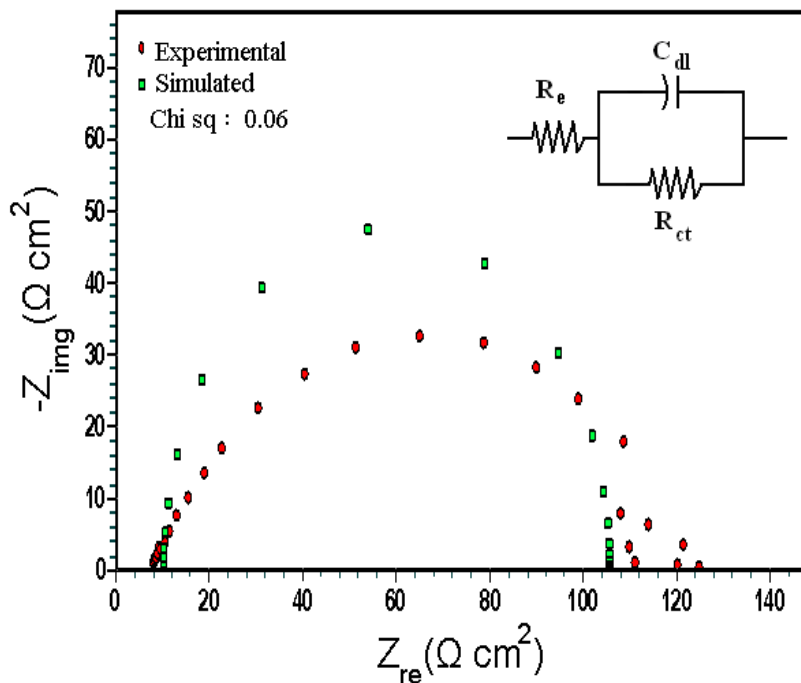


Figure 3. (B)

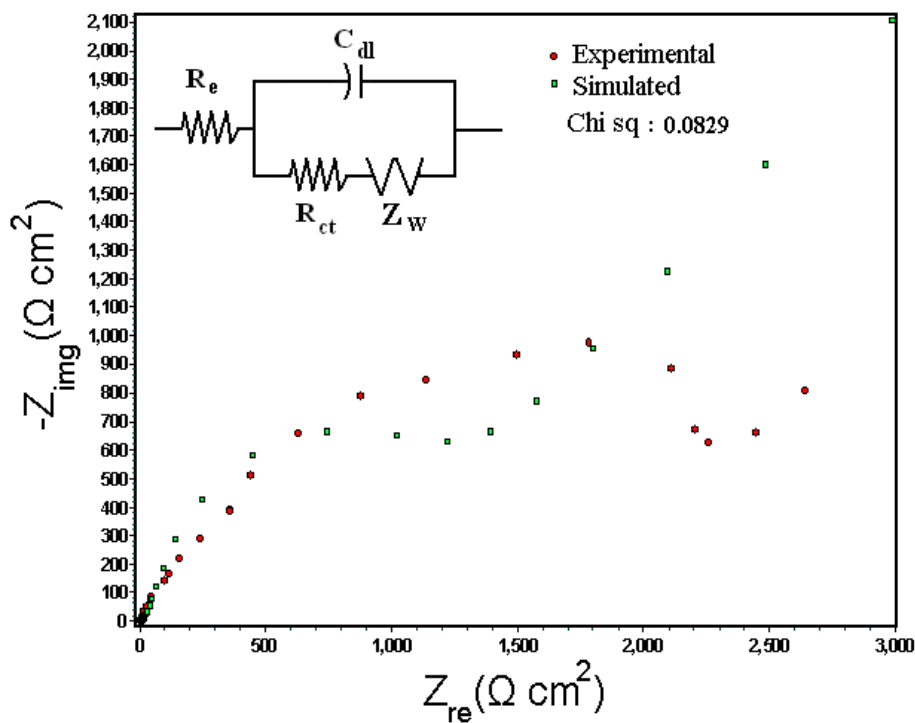


Figure 3. (C)

**Figure 3.** (A) Typical Potentiodynamic polarization curves of electrodeposited alloy and bare substrate in 3.5% NaCl solution. (B and C) Electrochemical impedance spectroscopy both (●) experimental and (■) simulated Nyquist plot for mild steel (MS) and Fe<sub>54.62</sub>Ni<sub>30.87</sub>.Cr<sub>14.5</sub> alloy on mild steel (Fe<sub>54.62</sub>Ni<sub>30.87</sub>.Cr<sub>14.5</sub> / MS) (insert Equivalent circuit diagrams for impedance spectra).

The lower the porosity values the better is corrosion protection and the less defects are in the alloy electrodeposits. The double layer capacitance parameter  $C_{dl}$  was another parameter that could provide information about the polarity and the amount of charge at the alloy deposits/solution interface. Higher  $E_{corr}$ ,  $R_{ct}$ ,  $Z_w$  and lower  $I_{corr}$ ,  $C_{dl}$  values of Fe<sub>54.62</sub>Ni<sub>30.87</sub>Cr<sub>14.5</sub> alloy electrodeposited on mild steel substrate showed better corrosion resistance properties than that of bare substrates.

#### 4. CONCLUSIONS

We developed a novel DES for the electrodeposition of Fe-Ni-Cr alloy without H<sub>2</sub> evolution. The major advantages of DES are free from Cr-complexing agent, brightener and stress reducer. The effect of electrodeposition potential on the structural morphology and composition of Fe-Ni-Cr alloy was successfully studied by SEM and EDAX techniques. From these results potential for electrodeposition of Fe-Ni-Cr alloy compositions is optimized. We obtained higher Cr% in alloy composition without Cr-complexing agent at -1.5V; whose structural morphology is fine grained dense nodular deposit. The Potentiodynamic polarization and Electrochemical Impedance Spectroscopy results showed Fe<sub>54.62</sub>Ni<sub>30.87</sub>Cr<sub>14.5</sub> alloy deposited at -1.5V is having very high  $R_{ct}$ ,  $Z_w$  and lower  $I_{corr}$  than that of bare mild steel substrate.

#### ACKNOWLEDGMENT

Authors thank the Department of Science and Technology New Delhi for a research grant under SERC (Engineering Sciences) scheme no. SR/S3/ME/ 0030/2009. We thank the Director, (CSIR)-CECRI to carryout the research work and Mr. R. Ravishanker CECRI for SEM and EDAX measurement.

#### References

1. E. Oberg, *Machinery's Handbook*, 25<sup>th</sup> ed.; Industrial Press Inc: New York, 1996, p. 411.
2. T.E. Harris, G.M. Whitney and I.M. Croll, *J. Electrochem. Soc.* 142 (1995) 1031.
3. P.C. Andricacos and N. Robertson, *IBM. J. Res. Dev.* 42 (1998) 671.
4. M.A. Ameer, A.M. Fekry, A.A.Ghoneim and F.A. Ataby, *Int. J. Electrochem. Sci.* 5 (2010) 1847.
5. L.T. Romankiw, *Electrochim. Acta.* 42 (1997) 2985.
6. M.R. El-Sharif, A. Watson and C.U. Chisholm, *Trans. IMF.* 66 (1988) 34.
7. M.R. El-Sharif, J. MacDougall and C.U. Chisholm, *Trans. IMF.* 77 (4) (1999) 139.
8. F. Wang and T. Watanabe, *Mater. Sci. Eng. A.* 349 (2003) 183.
9. H. Adelhani and MR Arshadi, *J. Alloys and Compounds.* 476 (2009) 234.
10. A.G. Dolati, M. Ghorbani and A. Afshar, *Surf. Coat. Technol.* 166 (2003) 105.
11. B.M. In, E. Akiyama, H. Habazaki, A. Kawashima, K. Asami and K. Hashimoto. *Corros. Sci.* 37 (1995) 709.
12. A.P. Abbott, G. Capper, D.L. Davies and R.K. Rasheed, *Chem. Eur. J.* 10 (2004) 3769.
13. A.M. El Sherik and U. J. Erb, *Mater. Soc.* 30 (1995) 5743.
14. S-H. Deng and Z-Q. Gong, *Anti-Corrosion Methods and Materials.* 50(4) (2003) 267.
15. S. N. Srimathi and S. M. Mayanna, *Mater. Chem. Phys.* 11 (1984) 351.

16. S. Surviliene, A. Lisowska-Oleksiak, A. Selskis and A. Cesuniene, *Trans. IMF*. 86 (5) (2006) 241.
17. A.P. Abbott, G. Capper, K.J. McKenzie and K.S. Ryder. *J. Electroanal. Chem.* 599 (2007) 288.
18. A.P. Abbott, J.C. Barron, K.S. Ryder and D. Wilson. *Chem. Eur. J.* 13 (2007) 6495.
19. M.V. Cardoso, S.T. Amaral and E.M.A. Martín, *Corros. Sci.* 50 (2008) 2429.
20. Y.P. Liu, Y. J. Zhu, Y.H. Zhang et al, *J Mater Chem.* 7(5) (1997) 787.
21. L. Xu, J. Du, S. Ge, N. He and S. Li, *J Appl Electrochem.* 39(5) (2009) 713.
22. L. Sziraki, E. Kuzmann, M. El-Sharif, C.U. Chisholm, G. Principi, C. Tosello and A. Vertes, *Electrochem. Commun.* 2 (2000) 619.
23. L. Philippe and C. Heiss, *J. Michler, Chem. Mater.* 20 (2008) 3377.
24. S. Abd El rehim, M. Ibrahim and M. Dankeria, *Trans. IMF*. 80 (2002) 29.
25. A.A. Kornyshev and M.A. Vorotyntsev, *J. Electroanal. Chem.* 167 (1984) 1.
26. A.A. Kornyshev, *Electrochim. Acta.* 12 (1989) 1829.
27. M. Bojinov, I. Betova and R. Raicheff, *J. Electroanal. Chem.* 430 (1997) 169.
28. N. Sato, *J. Electrochem. Soc.* 129 (1982) 255.
29. A.Y. Musa, A.A. H. Kadhun, A.B. Mohamad, A. R. Daud, M.S. Takriff, S. K. Kamarudin and N. Muhamad, *Int. J. Electrochem. Sci.* 4 (2009) 707.
30. Zaki Ahmad, *Principles of Corrosion Engineering and Corrosion Control*, Elsevier Science & Technology, 2006 (Chapter-4), p. 73.
31. J.R. MacDonald (Ed). *Impedance Spectroscopy*, Wiley, New York, 1987.
32. G. Saravanan and S. Mohan, *Corros. Sci.* 51 (2009) 197.
33. G. Saravanan and S. Mohan, *J Appl Electrochem.* 39 (2009) 1393.